Periodic orbit analysis of molecular vibrational spectra: 1:1 resonant coupled modes

Daniel C. Rouben and Gregory S. Ezra
Baker Laboratory, Department of Chemistry, Cornell University, Ithaca, New York 14853

(Received 28 March 1995; accepted 17 April 1995)

In this paper we analyze the quantum density of states for a model molecular vibrational Hamiltonian describing two coupled anharmonic (Morse) oscillators. Periods of classical periodic orbits as a function of energy and coupling parameter are extracted directly from the quantum spectrum using the Gabor transform. We are able to identify the quantum manifestation of the local-to-normal transition, and of resonant bifurcations of periodic orbits. © *1995 American Institute of Physics.*

I. INTRODUCTION

Understanding the nature of highly-excited vibrational and rotation-vibration states of polyatomic molecules is a problem of central importance in chemical physics.[1] In the standard procedures of spectroscopy, which have proved very successful for low-lying states of polyatomic molecules, rotation-vibration states are assigned full sets of good vibrational (normal mode) and rotational (rigid rotor) quantum numbers, and level patterns are fitted by varying parameters in a suitable effective spectroscopic Hamiltonian.[2] Problems arise in trying to extend these methods to analyze spectra involving highly-excited rotation-vibration states. Strong mode couplings due to anharmonic potential terms and rotation-vibration interactions in general render assignment of labels to individual quantum states problematic,[1] and level shifts and splittings mean that traditional spectroscopic pattern recognition techniques are no longer effective. The state-mixing induced by such coupling terms and the resulting complexity of the spectrum is a manifestation of the phenomenon of intramolecular vibrational energy redistribution (IVR).[3] Moreover, the large densities of states typically found for high levels of vibrational excitation may prevent resolution of individual spectral lines, so that standard fitting techniques based on line by line assignments no longer apply.

New approaches are therefore needed to go beyond the standard methods of spectroscopy in the strongly coupled regime. Recent work has included statistical Fourier transform spectroscopy,[4] the spectroscopy of clumps ,[5] bifurcation analysis and catastrophe maps,[6] hierarchical tree analysis,[7] periodic orbit approaches,[8] and analyses based on the semiclassical propagator.[9] A fundamental problem is to extract information on the underlying molecular Hamiltonian and associated dynamics from the observed spectrum.

The methods and concepts of semiclassical mechanics have been widely used in the theory of highly excited molecules.[10] Much work has been devoted to the problem of semiclassical quantization of molecular energy levels[11]; that is, computation of approximate quantum eigenvalues and eigenstates from classical mechanical information only.[10,12] Semiclassical quantization methods developed so far apply strictly only in either the integrable[13] or fully chaotic[14] limits. The intermediate case of a system exhibiting a generic mixed phase space with both regular and chaotic components is not yet well understood.

For integrable systems, individual semiclassical energy levels are obtained by quantization of the good actions associated with invariant tori (EBK quantization, see Refs. 11 and 13). For fully chaotic systems, invariant tori do not exist and EBK quantization is no longer applicable. Nevertheless, an approach to quantization of chaotic systems has been developed based on the properties of isolated unstable periodic orbits, which form an invariant skeleton of the phase space structure (cf. Ref. 15).

The procedure for quantization of chaotic systems exploits the Gutzwiller trace formula (GTF), which is a central result on the quantum-classical correspondence in the semiclassical limit.[16] The GTF expresses the quantum mechanical density of states in the $\hbar \to 0$ limit as a sum over isolated periodic orbits (pos). The quantum mechanical density of states

$$n(E) = \sum_{i=1}^{\infty} \delta(E - E_i) \tag{1.1}$$

is expressed in the semiclassical limit $\hbar \to 0$ as a po sum

$$n(E) = \bar{n}(E) + \Re\left[\sum_{p} \sum_{m=1}^{m=\infty} \tau_p(E) \frac{\exp[imS_p(E)/\hbar - im\mu_p\pi/2]}{\hbar\sqrt{|\det(M_p^m - 1)|}} \right]. \tag{1.2}$$

Here the subscript p specifies the po and the index m labels its mth repetition. The quantity $\bar{n}(E)$ is the mean level density, the contribution of the zero time orbits (i.e., the points of equilibrium), and is a smooth function of the energy E. The oscillatory part of the density of states is then a sum of contributions from all pos with period $\tau > 0$. In this primitive semiclassical version of the GTF, an individual periodic orbit p contributes to the sum with amplitude $1/\sqrt{|\det(M_p^m - 1)|}$, whose magnitude depends on the stability of the po. The stability (monodromy) matrix M_p describes the linearized dynamics in the vicinity of the po p. The matrix M_p has unit determinant, and its eigenvalues come in pairs $\exp[\pm\lambda]$ (for two degree-of-freedom systems). The quantity λ is real for unstable orbits and pure imaginary for stable pos. The amplitudes of unstable pos are given by

$1/\sqrt{|\det(M_p^m-1)|}=\sinh^{-1}(m\lambda/2)$ and so decay exponentially for $m\lambda$ large. For fully chaotic systems, all pos are unstable, and it is possible in some cases to develop symbolic codes to enumerate the pos in a systematic fashion.[16] On the other hand if a periodic orbit is stable the primitive semiclassical amplitude $1/\sqrt{|\det(M_p^m-1)|}=1/\sin(m\lambda/2)$ oscillates and diverges whenever $(m\lambda/2)=n\pi$, i.e., at a bifurcation point.[12] A classical bifurcation occurs when the eigenvalues $\exp[\pm m\lambda\tau]$ of the monodromy matrix M_p^m pass through unity, and is associated with a splitting or merging of two or more pos.[12] For parameter values (e.g., energy, coupling strength) close to the bifurcation point the relevant pos are not well separated in phase space so that the stationary phase approximations used in the derivation of Eq. (1.2) break down.[12] At resonant bifurcations, the eigenvalues of the linearized map M are of the form $\exp[2\pi in/m]$, m,n integer, and the central stable orbit gives birth to a rational torus characterized by winding number n/m.

To repair the deficiencies of the primitive semiclassical GTF (1.2) it is necessary to go beyond the stationary phase approximation and develop uniform semiclassical approximations that yield finite amplitudes near and at classical bifurcation points.[17] Several efforts have been made along these lines in recent years.[18,19]

For an integrable system, in which the phase space is filled with invariant tori, the semiclassical density of states can be described using either the EBK quantization condition[13] or, equivalently, the formula of Berry and Tabor, which expresses the density of states as a sum of contributions from rational or periodic *tori*.[20] The relation between the Berry-Tabor formula and the GTF po sum has been discussed by Ozorio de Almeida.[12,21]

We can formally evaluate the contribution to the quantum density of states from an individual periodic orbit p (stable or unstable) by computing the sum over repetitions m in Eq. (1.2). For an isolated unstable po, the sum over m gives a level density corresponding to equally spaced Lorentzian ''resonance'' peaks, with width determined by the instability exponent λ.[22] The sum for a stable po yields a quantization condition on the energy that is an approximation to the EBK quantization condition for tori in the vicinity of the stable po.[22]

The ''forward'' quantization problem then consists of numerical or analytical determination of periodic orbits and their properties followed by evaluation of the level density via Eq. (1.2). In principle, this process allows extraction of eigenvalues from information about the classical system alone. An essential difficulty with this method is that for real values of the energy the GTF is in general not absolutely convergent.[16,23] One must then truncate the periodic orbit sum at a given orbit length and so count only certain orbits and their repetitions. In recent years much work has been devoted to improving the convergence of the sum but in general the extraction of individual quantum eigenvalues from classical information is an unsolved problem (cf., for example Ref. 24). In the present paper, however, we shall use the GTF ''in reverse'' to extract information on the classical mechanics directly from the eigenvalues of a molecular vibrational Hamiltonian, and so avoid these fundamental convergence issues.

Whereas there are fundamental practical and theoretical difficulties associated with the po quantization program, the reverse process in which information on classical pos is extracted from quantum mechanics does not suffer from such problems. The connection between long-range fluctuations of the quantum density of states about the mean (Thomas–Fermi) value and classical pos established by the GFT is revealed by Fourier transformation of the quantum spectrum, which may at first sight appear to be highly irregular, but whose power spectrum will exhibit peaks at multiples of the periods (or actions) of the least unstable pos.[16] This approach has been applied to several problems, including the hydrogen atom in a magnetic field,[25] model two-electron systems,[26] and coupled quartic oscillators.[27]

In the present work we apply periodic orbit analysis to a model spectroscopic Hamiltonian describing a system of two anharmonic (Morse) oscillators coupled by a single 1:1 resonant interaction. We investigate the possibility of extracting information on the underlying classical mechanics from the quantum spectrum alone in a regime corresponding to a highly vibrationally excited molecule. We examine, in particular, how periodic orbit properties (evolution of periods with energy, bifurcation points, etc.) and corresponding evolution of the global phase space structure can be determined directly from the quantum spectrum. It is important to note that periodic orbit analysis can readily be applied to smoothed level densities, corresponding to spectra in which individual levels are not resolved.

The coupled oscillator Hamiltonian we use is a widely studied model for the stretching modes in nonlinear triatomic molecules (see, for example, the papers of Kellman and co-workers[28]). Semiclassical quantization of this Hamiltonian has been studied by Neshyba and Child, who compared the results of primitive EBK quantization with the rational torus quantization approach of Berry and Tabor.[29] Neshyba and Child also applied a uniform semiclassical quantization condition to compute quantum levels in the vicinity of the local/normal separatrix.[29] The coupled oscillator system studied is typical of molecular vibrational Hamiltonians in that it does not have the mechanical scaling property, i.e., the phase space structure changes in a nontrivial way with energy.[6] Our results therefore illustrate the application of periodic orbit analysis to a nonscaling system. Instead of taking the Fourier transform of the whole available quantum spectrum (cf. Refs. 25–27), it is necessary to use a window in energy; such an approach has been used by Baranger *et al.*[30]

To examine the correspondence between the numerical Fourier transform of the density of states and the evolution of the families of pos determined using classical mechanics, we construct plots of po period τ vs energy E or coupling parameter β. We can follow the evolution of pos on such diagrams constructed from the quantum spectrum alone, and compare the results with the corresponding classical mechanical results.

There has of course been much previous work on application of periodic orbit theory ideas to molecular vibrational

problems (cf. Ref. 8). The ultimate aim of the present line of research is to derive information on the (unknown) molecular Hamiltonian from experimental vibration-rotation spectra. Thus, it has been shown that po characteristic diagrams (constructed purely classically) serve to discriminate very effectively between different model potential surfaces.[31] In the same spirit, we propose that the basic period versus energy relationship for a small number of short pos as extracted from the quantum spectrum will be helpful in characterizing the molecular Hamiltonian.

II. MODEL SPECTROSCOPIC HAMILTONIAN

A. Classical Hamiltonian

The Hamiltonian we study describes two coupled anharmonic oscillators, and is expressed in terms of canonical variables $(I_1, I_2, \psi_1, \psi_2)$, where subscript i labels quantities for oscillator i. The classical Hamiltonian has the form:

$$H(I_1, I_2, \psi_1, \psi_2) = \omega_1 I_1 + \omega_2 I_2 - a_1 I_1^2 - a_2 I_2^2 + 2\beta\sqrt{I_1 I_2}\,\cos(\psi_1 - \psi_2). \tag{2.1}$$

In the $\beta = 0$ limit, the Hamiltonian (2.1) describes two uncoupled oscillators, each of which has the energy-action relation appropriate for a Morse potential, i.e.,

$$\mathscr{H} = \omega I - aI^2, \tag{2.2}$$

where, in terms of standard Morse parameters D (dissociation energy), m (mass), and α (exponent), we have $\omega = \sqrt{2D/m}\,\alpha$ and $a = \omega^2/4D$.

Interpretation of period vs energy and coupling parameter diagrams derived from quantum spectra requires investigation of the main families of periodic orbits of the classical system, Eq. (2.1). For this integrable system, it is possible to derive many properties of the fundamental periodic orbits analytically.

We note that the classical phase space structure and bifurcation diagrams for Hamiltonians of type (2.1) have been extensively studied by Kellman and co-workers,[6,28] who have introduced the useful concept of the *polyad phase sphere* (see below).

B. Classical periodic orbits

We shall only consider the symmetric case $\omega_1 = \omega_2 = \omega$, $a_1 = a_2 = a$. With appropriate parameters, this system is a model for the stretching modes in a symmetric triatomic molecule such as H_2O.[28] The generalization to the nonsymmetric case has been studied by Li, Xiao, and Kellman.[28]

The generating function,

$$F = (\psi_1 - \psi_2)J_1 + \tfrac{1}{2}(\psi_1 + \psi_2)J_2 \tag{2.3}$$

defines a canonical change of variables $(I_1, I_2, \psi_1, \psi_2) \rightarrow (J_1, J_2, \phi_1, \phi_2)$. In terms of the new variables the Hamiltonian (2.1) becomes

$$H = \omega J_2 - a(2J_1^2 + \tfrac{1}{2}J_2^2) + 2\beta(\tfrac{1}{4}J_2^2 - J_1^2)^{1/2}\cos\phi_1. \tag{2.4}$$

This Hamiltonian describes the case where the two oscillators are identical and coupled by a 1:1 resonant interaction. The new angle $\phi_2 = \frac{1}{2}(\psi_1 + \psi_2)$ is ignorable so that the conjugate variable $J_2 = I_1 + I_2$ is a constant of the motion. The problem is therefore essentially one-dimensional. We can fix the energy E and plot level curves of J_2 in the (J_1, ϕ_1) plane. In Fig. 1 we show the evolution of phase space structure with coupling parameter β at fixed energy, $E = 20.0$. Other parameters are $\omega = 0.25$, $a = 0.000\,25$. In Fig. 2, we show the evolution of phase space structure with energy E at fixed $\beta = 0.01$. We take $\omega = 0.5$, $a = 0.001$ in these plots.

1. Uncoupled limit

We now consider the periodic orbit structure in the uncoupled limit $\beta = 0$. Analytical results obtained in this limit will be useful in interpreting results obtained for the coupled system.

For $\beta = 0$ the Hamiltonian (2.1) is

$$H^0 = \omega(I_1 + I_2) - a(I_1^2 + I_2^2). \tag{2.5}$$

This Hamiltonian is independent of the angles ψ_1 and ψ_2 and the entire phase space is filled with tori; there are no unstable pos. We can easily find the periods of orbits lying on commensurable (rational) tori. The frequencies on the two-torus are given by $\Omega_1 = (\partial H^0/\partial I_1)$ and $\Omega_2 = (\partial H^0/\partial I_2)$. For a rational torus, we have $\Omega_1/\Omega_2 = n_1/n_2$, with n_1, n_2 integers. The action of a po on this $n_1{:}n_2$ commensurable torus is then

$$\mathscr{J} = n_1 I_1 + n_2 I_2, \tag{2.6}$$

where I_2 and I_1 are the individual oscillator actions for the rational torus at the chosen energy E. The corresponding period is given by the derivative $(\partial \mathscr{J}/\partial E)$ with the ratio n_1/n_2 held constant. Using Eq. (2.5) we obtain after some manipulation,

$$\tau(n_1, n_2, E) = \sqrt{\frac{n_1^2 + n_2^2}{2\omega^2 - 4aE}}. \tag{2.7}$$

2. Nonzero coupling

We now consider the case of nonzero bond coupling, $\beta > 0$. Let $\mathscr{T}: \Sigma \rightarrow \Sigma$ denote the Poincaré map of the (J_1, ϕ_1) plane Σ onto itself induced by motion under one period of the ϕ_2 motion. As ϕ_2 is ignorable, the map $\mathscr{T}$ is independent of the particular value of ϕ_2 used to define the surface of section. Therefore the fundamental pos, which are associated with fixed points of $\mathscr{T}$, can be obtained analytically by finding the roots of the set of equations,

$$\dot{\phi}_1 = \frac{\partial H}{\partial J_1} = 0, \quad \dot{J}_1 = -\frac{\partial H}{\partial \phi_1} = 0. \tag{2.8}$$

We find four such fundamental (period-one) fixed points of the map $\mathscr{T}$, labeled fp(1), fp(2), fp(3), and fp(4). The fixed point fp(4) is just the reflection through the $J_1 = 0$ line of fp(3) and has the same period and action. The positions of the pos in the (J_1, ϕ_1) plane are

$$\text{fp(1)}: \quad \phi_1 = 0, \quad J_1 = 0, \tag{2.9a}$$

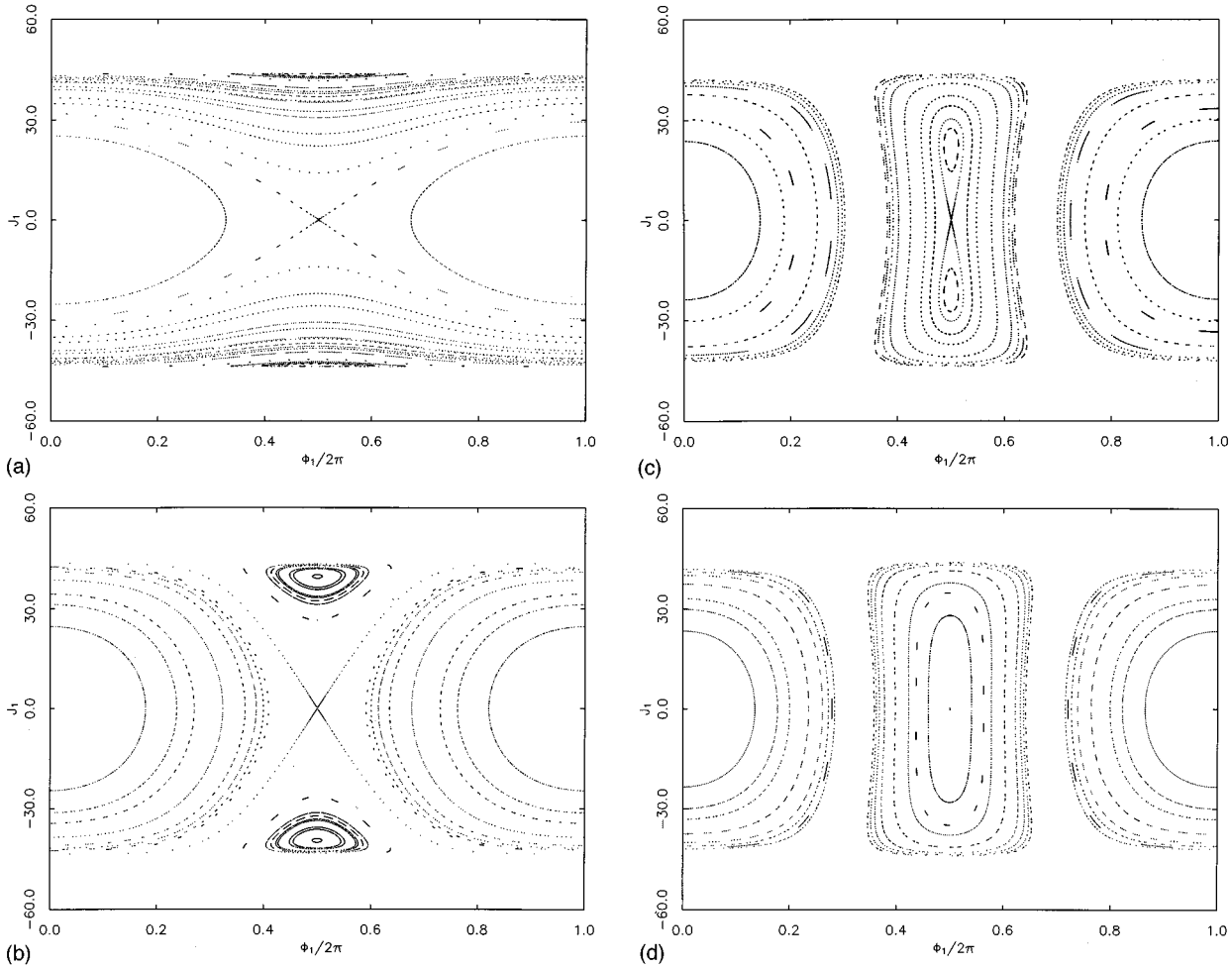

FIG. 1. Evolution of phase space structure with coupling parameter β, at fixed energy, $E=20.0$. Other parameters are $\omega=0.25$, $a=0.000\,25$. (a) $\beta=0.01$; (b) $\beta=0.02$; (c) $\beta=0.0225$; (d) $\beta=0.025$.

$$\text{fp(2)}: \quad \phi_1=\pi, \quad J_1=0, \tag{2.9b}$$

$$\text{fp(3), fp(4)}: \quad \phi_1=\pi, \quad J_1^2=\tfrac{1}{4}\left(J_2^2-\frac{\beta^2}{a^2}\right). \tag{2.9c}$$

To find the action of the corresponding orbits we substitute the values of ϕ_1 and J_1 corresponding to the fixed points into Eq. (2.4) and solve for J_2 at given E. The expressions for the actions J_2 of the fixed points are valid for all parameter and energy values,

$$\text{fp(1)}: \quad J_2=a^{-1}\{(\omega+\beta)-\sqrt{[}(\omega+\beta)^2-2aE]\}, \tag{2.10a}$$

$$\text{fp(2)}: \quad J_2=a^{-1}\{(\omega-\beta)-\sqrt{[}(\omega-\beta)^2-2aE]\}, \tag{2.10b}$$

$$\text{fp(3), fp(4)}: \quad J_2=a^{-1}\{\omega-\sqrt{[}\omega^2-4aE-2\beta^2]\}. \tag{2.10c}$$

The period of each orbit is found by calculating $(\partial H/\partial J_2)$. The results are

$$\text{fp(1)}: \quad \tau_1=\sqrt{[}(\omega+\beta)^2-2aE]^{-1}, \tag{2.11a}$$

$$\text{fp(2)}: \quad \tau_2=\sqrt{[}(\omega-\beta)^2-2aE]^{-1}, \tag{2.11b}$$

$$\text{fp(3), fp(4)}: \quad \tau_3=\sqrt{[}\omega^2-4aE-2\beta^2]^{-1}. \tag{2.11c}$$

Note that the periods of the orbits fp(1) and fp(2) from Eq. (2.11) both reduce to the result 2.7 with $n_1=n_2=1$ in the limit $\beta=0$.

Computation of the eigenvalues of the fixed point stability matrices,

$$\mathscr{M}=\begin{bmatrix} \dfrac{\partial^2 H}{\partial\phi_1\partial\phi_1} & \dfrac{\partial^2 H}{\partial\phi_1\partial J_1} \\ \dfrac{\partial^2 H}{\partial J_1\partial\phi_1} & \dfrac{\partial^2 H}{\partial J_1\partial J_1} \end{bmatrix} \tag{2.12}$$

shows that the fixed point fp(1) is stable for all a, β, and E. The fixed points fp(3) and fp(4) are stable when they exist. The fixed point fp(2) changes its stability as parameters are varied. As β is increased at fixed a, for example, a critical point is reached at which the stable "polar" fixed points fp(3) and fp(4) merge with fp(2) to form a single stable fixed point at $\phi_1=\pi, J_1=0$ in a symmetric isochronous pitchfork bifurcation[32] [cf. Figs. 1(c), and 1(d)]. The resulting fixed point remains stable as β is increased further. Equating the periods (2.11b) and (2.11c) yields an equation relating the critical values of a and β at given E

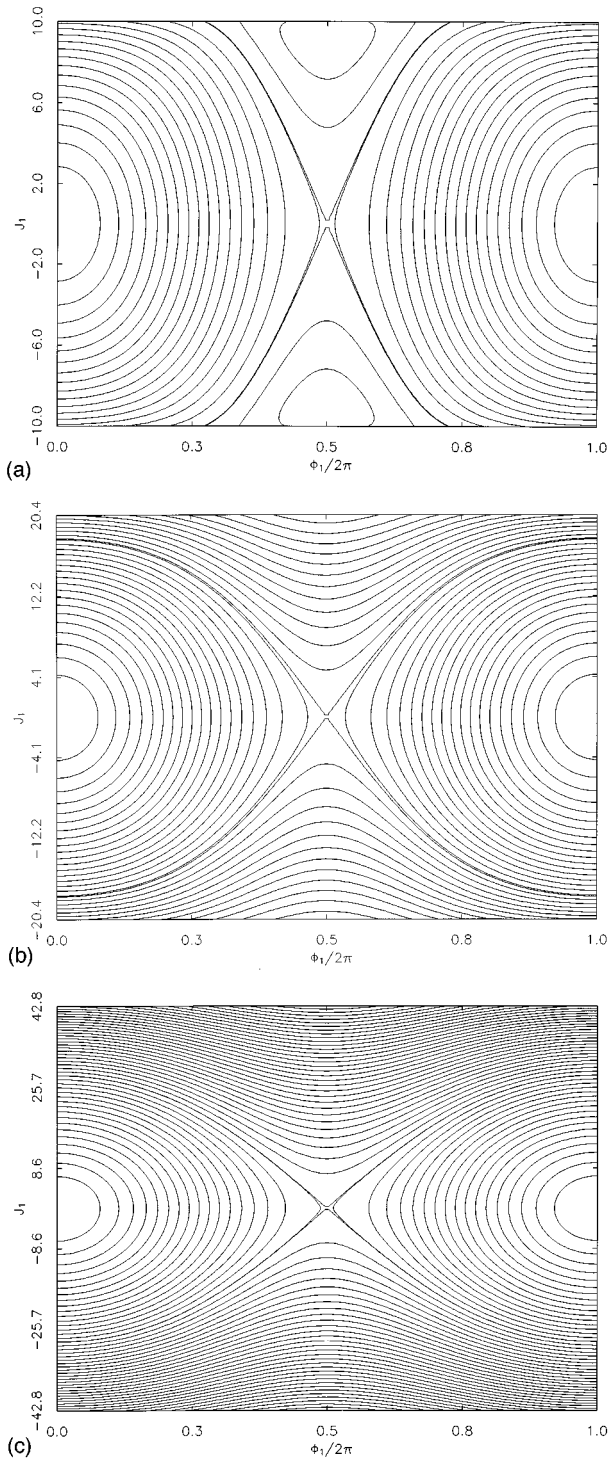

FIG. 2. Evolution of the phase space structure with energy E at fixed coupling parameter $\beta=0.01$. Other parameters are $\omega=0.5$, $a=0.001$. (a) $E=10.0$; (b) $E=20.0$; (c) $E=40.0$.

$$3\beta^2-2\beta\omega+2aE=0. \tag{2.13}$$

We can either solve for the critical parameter β^{**} as a function of E, ω, and a, or a^{**} as a function of E, ω and β. We have,

$$\beta^{**}=\frac{\omega^2-\sqrt{(\omega^2-6aH)}}{3}, \tag{2.14a}$$

$$a^{**}=\frac{\omega\beta}{H}-\frac{3\beta^2}{2}. \tag{2.14b}$$

Since the Hamiltonian (2.1) is effectively one-dimensional, a global view of the classical phase space structure is easily obtained. The structure of the Poincaré section at fixed E is best understood by plotting it on the surface of a sphere [33]; the closely related polyad phase sphere of Kellman and coworkers is obtained when level curves of $H(J_1,\phi_1;J_2)$ are plotted on a sphere at constant J_2.[6,28] Coordinates on the sphere are ϕ_1, the usual polar angle ϕ, and J_1, the z-coordinate. The surface of the (constant E) sphere is then filled with level curves of J_2.

For the parameter values of Fig. 1(a), for example, the phase space consists of a resonance zone in the equatorial region of the sphere and two regions filled with nonresonant tori in the vicinity of the poles [fp(3) and fp(4)]. The resonance zone is filled with *normal mode* trajectories, whereas the nonresonant trajectories are *local mode*.[34] A separatrix defined by the action $J_2=\{\omega-\beta-\sqrt{[(\omega-\beta)^2-2aH]}\}/a$ separates the local and normal mode regions. We cannot determine the actions or periods of rational tori in either the local or normal mode regions analytically; for small values of β, the actions of rational local mode tori can however be found approximately by setting $\beta=0$ and proceeding as before to get Eq. (2.6).

Figure 1 shows the evolution of the global structure of the constant E phase sphere with changes in parameter β. For values of β above β^{**} [Fig. 1(d)], the whole sphere is covered by a single family of resonant tori bounded by two stable fixed points at $\phi=0,J_1=0$ and $\phi=\pi,J_1=0$. This is the pure normal mode limit.

C. Quantum mechanical Hamiltonian

The quantum counterpart of the classical Hamiltonian (2.1) is obtained using the well-known correspondence between action-angle variables and creation-annihilation operators,[6]

$$\hat{a}^\dagger\leftrightarrow J^{\frac{1}{2}}e^{i\phi},\quad \hat{a}\leftrightarrow J^{\frac{1}{2}}e^{-i\phi}. \tag{2.15}$$

In terms of creation and annihilation operators, the 1:1 coupling term is $\beta(\hat{a}_1^\dagger\hat{a}_2+\hat{a}_1\hat{a}_2^\dagger)$, and the quantum Hamiltonian matrix in a basis of number states $|n_1,n_2\rangle$ takes the form,

$$\begin{aligned}H_{\bar{n}_1,\bar{n}_2;\,n_1,n_2}=&[\omega(n_1+\tfrac{1}{2})+\omega(n_2+\tfrac{1}{2})-a(n_1+\tfrac{1}{2})^2\\&-a(n_2+\tfrac{1}{2})^2]\delta^-_{\bar{n}_1,n_1}\delta^-_{\bar{n}_2,n_2}+\beta\sqrt{[n_1(n_2+1)]}\\&\times\delta^-_{\bar{n}_1,n_1-1}\delta^-_{\bar{n}_2,n_2+1}+\beta\sqrt{[(n_1+1)n_2]}\\&\times\delta^-_{\bar{n}_1,n_1+1}\delta^-_{\bar{n}_2,n_2-1}.\end{aligned} \tag{2.16}$$

The quantum Hamiltonian (2.16) conserves the total number of quanta (n_1+n_2), so that together with the energy there are two integrals of the motion and the quantum system is integrable. Diagonalization of the quantum Hamiltonian (2.16) in a basis of number states $|n_1,n_2\rangle$ gives the quantum level spectrum. Because of the integrability of the quantum

Hamiltonian, we are able to diagonalize matrices corresponding to each polyad independently (a polyad is defined by a particular value of $\mathcal{N}=n_1+n_2+1$).

Note that addition of other coupling terms, e.g., 2:1 coupling of the form $\hat{a}_1^\dagger \hat{a}_1^\dagger \hat{a}_2$, destroys the integrability of the problem. Although analysis of such a nonintegrable system is our ultimate goal, the present work treats the simplest case in which there is only a 1:1 coupling term.

III. PERIODIC ORBIT ANALYSIS OF THE QUANTUM DENSITY OF STATES

A. Gabor transform of the density of states

For scaling systems (i.e., systems with potential functions homogeneous in coordinates) the classical phase space structure is effectively independent of energy.[16] Periodic orbit actions and periods have a simple dependence on energy, and it is possible to express the density of states in terms of a reduced energy ε, such that po actions are proportional to ε.[16] Information on the quantum density of states at *all* available energies E can then be used to determine the po decomposition of the density of states.[25–27] Moreover, an analysis of the classical phase space need only be done at a single value of the energy.

In nonscaling systems, such as typical molecular vibrational Hamiltonians, the phase space structure has a nontrivial E-dependence, as do the po actions, periods and stability parameters. To obtain information on the classical dynamics from the quantum spectrum, it is necessary to analyze the density of states in the vicinity of a particular energy value $\bar{E}$; one obvious possibility is to multiply the density of states by a window function centered at $\bar{E}$. Meredith *et al.* have in fact shown that the Fourier transform of the quantum density of states with respect to E obtained using a Gaussian window centered at some chosen energy $\bar{E}$ contains peaks associated with classical pos at the same chosen energy.[30] Use of a Gaussian window of width ΔE corresponds to taking the *Gabor transform* of the density of states,[35]

$$G_{\bar{E}}(t)=\int_{-\infty}^{\infty}\exp\left[\frac{-(E-\bar{E})^2}{2\Delta E^2}\right]\exp\left(\frac{-iEt}{\hbar}\right)\times \mathrm{Tr}[\,\delta(E-\hat{H})]\,dE$$
$$=\sum_n \exp\left[\frac{-(E_n-\bar{E})^2}{2\Delta E^2}\right]\exp\left(\frac{-iE_nt}{\hbar}\right). \tag{3.1}$$

The power spectrum is then simply $|G_{\bar{E}}(t)|^2$. In the semiclassical limit $\hbar\to 0$, we can substitute the GTF for the density of states into Eq. (3.1); after expanding the E-dependent exponent about $\bar{E}$, we obtain a power spectrum with peaks centered at the *periods* τ of classical pos at the energy $\bar{E}$. Nevertheless, because we must limit the energy range in the Fourier transform to an interval of width ΔE about $\bar{E}$, the determination of classical po periods is in general not as precise as in the case of scaling systems.

Computation of the power spectrum $|G_{\bar{E}}(t)|^2$ at many values of $\bar{E}$ yields an energy vs period (E,τ) plot, which can be compared with the corresponding classical result.[30] In like fashion, we can also study evolution of periodic orbit periods with β (fixed $\bar{E}$, a) and a (fixed β, $\bar{E}$). Of particular interest is the manifestation of classical bifurcations and resonances.

Note that we can reduce the effective value of $\hbar$ and hence increase the density of states at fixed E by the following scalings:

$$\omega\to\bar{\omega}=\omega/c,\ a\to\bar{a}=a/c^2,\ \beta\to\bar{\beta}=\beta/c,\ \hbar\to\bar{\hbar}=\hbar/c. \tag{3.2}$$

B. Contribution of pos and rational tori to the density of states

In the previous section we determined analytically the locations of the fundamental (period-one) families of periodic orbits. These fundamental orbits contribute to the density of states in the manner described by the GTF, Eq. (1.2). There will moreover be contributions to the density of states from rational tori in the local and normal mode regions, as described by the Berry and Tabor formula.[20] A given commensurability condition on the torus frequencies can in general only be satisfied by *real* (as opposed to complex) trajectories for limited ranges of energy or parameter values. Outside the physical parameter range, it may still be possible to satisfy the commensurability condition on *complex* tori; such tori still contribute to the density of states, albeit with a higher power law dependence on $\hbar$ than real tori.[20] Uniform semiclassical analysis shows that the associated action is a multiple of the action of the po that lies at the boundary of the physical action space,[20] so the net result is a peak in the power spectrum at a multiple of the period of the boundary po.

In the present problem, the stable fixed points represent the border between the real and complex regions for the rational tori; that is, rational tori appear by resonant bifurcation of the stable pos. High-order resonances are manifested in the divergence of the primitive semiclassical amplitudes of fp(1) or fp(2) [after merging with fp(3)] in the po sum, and occur when the eigenvalues of the monodromy matrix for these fixed points are of the form $\exp[\pm in2\pi/m]$.

IV. ANALYSIS OF QUANTUM (β,τ) AND (E,τ) PLOTS

Using the Gabor transform method described above we have constructed (E,τ) diagrams from the quantum density of states at fixed coupling parameter β as well as β vs τ plots for fixed energy E.

A. Quantum (β,τ) plots

1. Local to normal transition

Consider first variation of the coupling parameter β at fixed energy E. A quantum (β,τ) plot is shown in Fig. 3 for energy $\bar{E}=20.0$. (Recall that E is the energy at the center of the Gaussian window in energy space.) We take $\omega=0.25$, $a=0.000\,25$ (cf. Fig. 1). The (β,τ) plot in Fig. 3 clearly reflects the various bifurcations involving the fundamental pos, and we can easily trace the evolution of peaks associated with (multiple) periods of the major pos. The range of τ plotted includes the second, third, and fourth repetitions of the fundamental pos.

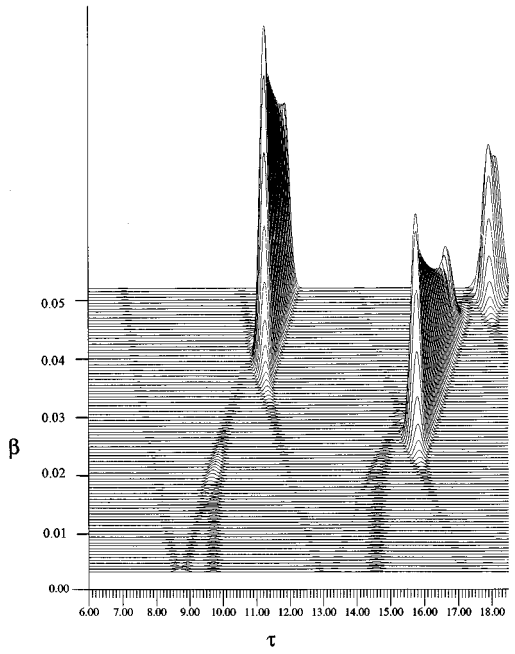

FIG. 3. Quantum (β,τ) plot. The coupling parameter β is varied at fixed energy $E=20.0$. We take $\omega=0.25$, $a=0.000\,25$ (cf. Fig. 1). The Gaussian width $\Delta E=1.2$. Coupling parameter β ranges from 0.0035 to 0.052.

At $\beta=0$, the periods of the stable and unstable periodic orbits corresponding to fp(1) and fp(2), respectively, are equal ($\tau=4.36$). As β increases from zero, the two periods split apart, and this splitting can be seen very clearly at small β values. Close in period to the initially isochronous fp(1) and fp(2) orbits are the stable pos fp(3) and fp(4) ($\tau=4.85$ for $\beta=0$). As β increases these pos move towards the equator of the phase sphere until they merge with the unstable po fp(2) to yield a single stable po. A detailed uniform semiclassical analysis of this symmetric isochronous inverse pitchfork bifurcation has recently been given.[19] The associated merging of peaks is evident in Fig. 3. We note that the β value at which peak merging occurs is shifted slightly away from the actual classical bifurcation point, $\beta^{**}=0.0232$[19]; this shift is analogous to the displacement of the rainbow maximum in the quantum differential cross section away from the classical rainbow angle in ordinary potential scattering.[36]

For β values greater than the classical bifurcation point $\beta=\beta^{**}$, the system is in the normal mode regime, with fp(1) $\equiv$ ''symmetric stretch'' and fp(2) $\equiv$ ''asymmetric stretch'' pos. The local to normal transition can therefore be observed through analysis of the Gabor transform of the density of states.

2. Resonant bifurcations and rational tori

At certain β values larger than β^{**}, the value at which the phase sphere is completely filled with normal mode tori, the amplitudes of peaks associated with various multiples of the period of the stable po fp(1) increase rapidly.

A high order resonance involving the stable po fp(1) occurs when the eigenvalues of its monodromy matrix are of the form $\exp[\pm i2\pi n/m]$, n,m integer. The primitive semiclassical version of the GTF predicts that the associated amplitude in the po sum for the density of states diverges at such points. The observed rapid increase and decrease in the amplitude of peaks associated with fp(1) is a smoothed manifestation of this divergence. Computation of the stability matrix of the fixed point fp(1) shows that resonant bifurcations of the multiples $(m+1)\times$fp(1) seen in Fig. 3 are associated with $m+1:1$ commensurabilities between the frequency of the central orbit fp(1) and that of rotation about the po.

At the resonant bifurcation an $m+1:1$ rational torus appears; the peak associated with this torus splits off from the $(m+1)\times$fp(1) peak, and is associated with the contribution to the density of states expected from the Berry–Tabor formula.[20] The $m+1:1$ rational torus peak eventually merges with the $m\times$fp(2) peak at larger β. Pictured in terms of the phase sphere, the $m+1:1$ rational torus splits off from the fp(1) po, moves over the sphere and merges with the fp(2) po at the antipodal point in an inverse $m:1$ resonant bifurcation.

The results of Ref. 37 provide additional insight into the properties of rational tori in the phase space of Hamiltonian (2.1). In that paper, a detailed discussion of the classical, semiclassical and quantum mechanics of 1:1 resonantly coupled *harmonic* oscillators was given. Specifically, it was shown that, in the harmonic $(a=0)$ limit, the classical Hamiltonian (2.4) can be written as

$$H=\omega J_2+\beta K, \tag{4.1}$$

where K is a new action variable obtained by a canonical transformation whose generating function is given in Ref. 37. The action variable K satisfies $-J_2\leqslant K\leqslant J_2$.

The action K provides a label (in addition to the constant of the motion J_2) for invariant tori in the harmonic limit of Eq. (2.4). These tori form a one-parameter family, where fixed points fp(1) and fp(2) correspond to $K=J_2$, $K=-J_2$, respectively, and the action variable K provides a continuous parameterization of the family of tori. In order to discuss frequency commensurabilities (winding numbers), it is necessary to label the invariant tori with an action variable that vanishes at either fixed point. We therefore define a *pair* of canonical transformations $(J_2,K,\phi_2,\phi_K)\rightarrow(J,\mathscr{A}_\pm,\phi_J,\phi_{\mathscr{A}_\pm})$ by the generating functions,

$$G_\pm=\phi_J J_2+\tfrac{1}{2}\phi_{\mathscr{A}_\pm}(J_2\pm K), \tag{4.2}$$

giving

$$J=J_2,\ K=\pm(2\mathscr{A}_\pm-J_2). \tag{4.3}$$

In terms of the new variables, the Hamiltonian (4.1) is

$$H=(\omega\mp\beta)J\pm 2\beta\mathscr{A}_\pm. \tag{4.4}$$

The actions $\mathscr{A}_\pm$ are just the phase space areas

$$\mathscr{A}_\pm=\frac{1}{2\pi}\oint d\phi_1\ J_1(E,J_2) \tag{4.5}$$

enclosed by invariant curves in the (J_1,ϕ_1) section surrounding the relevant fixed points. The action variable $\mathscr{A}_+=\frac{1}{2}(J+K)$ vanishes at the fixed point fp(2) $(J_2=-K)$, and serves to label invariant tori on the fp(2) half of the phase sphere $(0\leqslant\mathscr{A}_+\leqslant J)$, whereas the action variable

$\mathscr{A}_- = \frac{1}{2}(J-K)$ vanishes at fp(1) ($J_2 = K$), and labels tori on the fp(1) half of the sphere ($0 \leqslant \mathscr{A}_- \leqslant J$). The two sets of tori parametrized by the two action pairs have a single common element, the torus with $2\mathscr{A}_+ = 2\mathscr{A}_- = J$, $K = 0$.

On each side of the sphere, the action $\mathscr{A}$ is associated with motion "transverse" to the po corresponding to the relevant fixed point. Frequencies are

$$\omega_J \equiv \frac{\partial H}{\partial J} = \omega \mp \beta, \tag{4.6a}$$

$$\omega_{\mathscr{A}_\pm} \equiv \left| \frac{\partial H}{\partial \mathscr{A}_\pm} \right| = 2\beta, \tag{4.6b}$$

with ratio (winding number)

$$\rho_\pm = 2\beta/(\omega \mp \beta), \tag{4.7}$$

independent of actions. Therefore, at the β value for which the winding number on one side of the phase sphere is a rational number

$$\rho_- = 2\beta(\omega+\beta)^{-1} = 1/(m+1), \tag{4.8}$$

m integer, the winding number on the other side of the phase sphere is

$$\rho_+ = 2\beta(\omega-\beta)^{-1} = 1/m, \tag{4.9}$$

i.e., also a rational ratio.

In the full Hamiltonian, Eq. (2.1), the two oscillators are no longer harmonic, so that winding numbers are no longer constant on each half of the sphere. Nevertheless, the above result makes plausible the fact that an $(m+1)$:1 rational torus on one side of the sphere connects with an m:1 rational torus on the other (cf. Fig. 3). Qualitatively similar behavior to that seen in Fig. 3 can in fact be obtained using a model Hamiltonian,[38]

$$H' = \omega J_2 + \beta K + \gamma J_2 K, \tag{4.10}$$

where the parameter γ is a measure of nonlinearity. [We note that action-angle variables for the full Hamiltonian (2.1) have been found analytically by Joyeux[39]; the resulting expressions are extremely complicated, and cannot readily be used to obtain explicit expressions for, e.g., winding numbers.]

In summary, two major aspects of the classical dynamics are reflected in the quantum (β,τ) plots,

(1) The merging of the stable polar pos with the unstable fixed point fp(2) in an inverse symmetric isochronous pitchfork bifurcation. This merging marks the transition to the normal mode regime.
(2) Emergence of $m+1$:1 rational tori by resonant bifurcations of the stable po fp(1). These rational tori, which contribute to the density of states as per the Berry-Tabor formula, then evolve with increasing β to merge with the (stable) fixed point fp(2) in an m:1 resonance.

B. Quantum (E,τ) plot

In Fig. 4 we show a quantum (E,τ) plot obtained by fixing the coupling parameter $\beta = 0.01$ and sweeping the center of the Gaussian window in the Gabor transform over a range of energies. For this plot we use parameter values $\omega = 0.5$ and $a = 0.001$ (cf. Fig. 2).

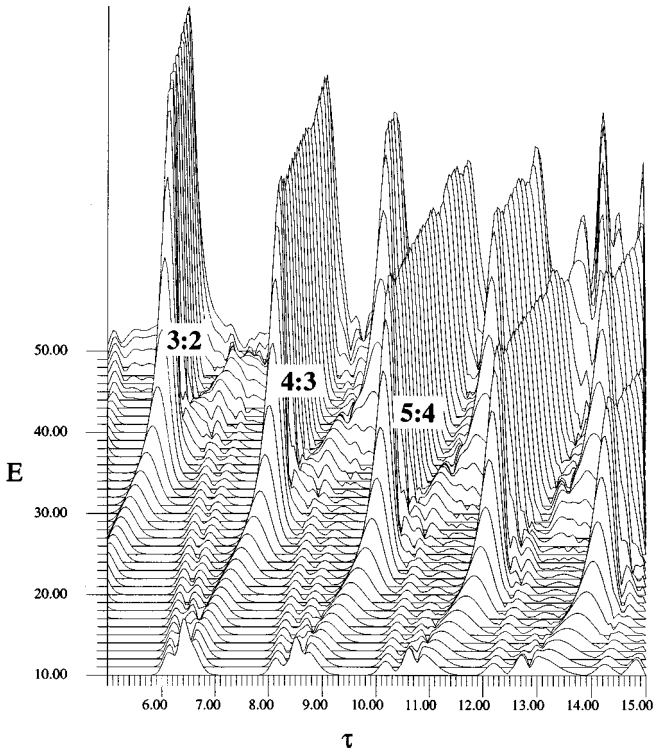

FIG. 4. Quantum (E,τ) plot. The energy at the center of the Gaussian window, E, is varied at constant coupling parameter $\beta = 0.01$ from 10.0 to 50.0. The Gaussian width $\Delta E = 2.0$. We take $\omega = 0.5$, $a = 0.001$ (cf. Fig. 2). The square root of the power spectrum is plotted to accentuate the contribution from smaller peaks.

With β fixed, the difference between the periods of pos fp(1) and fp(2) changes slowly with E; the associated (E,τ) traces are essentially parallel over the whole E range of interest. (The range of τ values shown includes the third to the sixth repetitions of the fundamental pos.) The po fp(2) is not involved in a pitchfork bifurcation for the E range studied.

The dominant features of the quantum (E,τ) plot of Fig. 4 are the rapid increases in peak heights associated with resonant bifurcations of the stable pos fp(3) and fp(4). As discussed above, resonant tori appear at such bifurcations and the corresponding peaks split off as β increases. For small β values we can approximately determine the E vs τ relation for resonant tori using Eq. (2.7), and so assign the observed peaks. The n_1:n_2 values for the dominant resonances in Fig. 4 form a sequence $m+1$:m (3:2, 4:3, 5:4, etc.).

V. CONCLUSIONS

We have applied periodic orbit theory to analyze the quantum density of states for a system of two anharmonic oscillators coupled by a 1:1 resonant coupling. Using the Gabor transform technique of Baranger *et al.*,[30] we have constructed (β,τ) and (E,τ) diagrams directly from the quantum level spectrum. We were able to correlate many features of these plots with corresponding features of the classical

phase space structure. In particular, we were able to recognize the quantum manifestation of the classical inverse symmetric pitchfork bifurcation that signals the onset of the normal mode regime. The effects of resonant bifurcations were also noted. The effects of dynamical tunneling,[40] which gives rise to exponentially small level splittings, are not revealed by our analysis.

There are several directions for future work. First of all, one would like to add further resonant coupling terms (e.g., 2:1) to the Hamiltonian, thereby breaking the integrability. A second direction is the addition of another degree of freedom, i.e., a bending mode. The classical-quantum correspondence for 3-mode systems has hardly been studied (see, however, Ref. 41). Finally, one ultimate aim of our work is to use the information on the fundamental pos obtained from the quantum (E,τ) plots as an aid to determining the spectroscopic Hamiltonian $\hat{H}$; the extent to which a potential function can be refined using (E,τ) plots remains to be determined.[42]

ACKNOWLEDGMENTS

This work supported by NSF Grant No. CHE-9403572. D.C.R. was supported by a NSERC Fellowship (PGS-A award No. 155665). We are grateful to Dr. K.M. Atkins for help with plotting.

[1] C.E. Hamilton, J.L. Kinsey, and R.W. Field, Annu. Rev. Phys. Chem. **37**, 493 (1986).
[2] D. Papousek and A.R. Aliev, *Molecular Vibrational-Rotational Spectra* (Elsevier, New York, 1982).
[3] See, K.K. Lehmann, G. Scoles, and B.H. Pate, Annu. Rev. Phys. Chem. **45**, 241 (1994), and references therein.
[4] J.P. Pique, J. Opt. Soc. Am. B **7**, 1816 (1990).
[5] R.W. Field, S.L. Coy, and S.B. Solina, Prog. Theor. Phys. Suppl. **116**, 143 (1994).
[6] M.E. Kellman, in *Molecular Dynamics and Spectroscopy by Stimulated Emission Pumping*, edited by H.-L. Dai and R.W. Field (World Scientific, Singapore, 1995).
[7] M.J. Davis, Chem. Phys. Lett. **192**, 479 (1992); J. Chem. Phys. **98**, 2614 (1993); in *Molecular Dynamics and Spectroscopy by Stimulated Emission Pumping*, edited by H.-L. Dai and R.W. Field (World Scientific, Singapore, 1995).
[8] J.M. Gomez Llorente, S.C. Farantos, O. Hahn, and H.S. Taylor, J. Opt. Soc. B **7**, 1851 (1990); R. Schinke, K. Weide, B. Heumann, and V. Engel, Faraday Discuss. Chem. Soc. **91**, 31 (1991); J.M. Gomez Llorente and E. Pollak, Annu. Rev. Phys. Chem. **43**, 91 (1992); S.C. Farantos, in *Time-Dependent Molecular Quantum Dynamics*, edited by J. Broeckhove and L. Lathouwers (Plenum, New York, 1992).
[9] E.J. Heller, in Chaos in Quantum Physics, edited by M.-J. Giannoni, A. Voros, and J. Zinn-Justin (Elsevier, New York, 1991); M.A. Sepulveda and E.J. Heller, J. Chem. Phys. **101**, 8004, 8016 (1994).
[10] M.S. Child, *Semiclassical Mechanics with Molecular Applications* (Oxford University, Oxford, 1991).
[11] See, for example, G.S. Ezra, C.C. Martens, and L.E. Fried, J. Phys. Chem. **91**, 3721 (1987), and references therein.
[12] A.M. Ozorio de Almeida, *Hamiltonian Systems: Chaos and Quantization* (Cambridge University, Cambridge, 1988).
[13] I.C. Percival, Adv. Chem. Phys. **XXXVI**, 1 (1977).
[14] See, for example, G.S. Ezra, K. Richter, G. Tanner, and D. Wintgen, J. Phys. B **24**, L413 (1991).
[15] P. Cvitanovic, Physica D **51**, 138 (1991).
[16] M. Gutzwiller, *Chaos in Classical and Quantum Mechanics* (Springer, New York, 1990).
[17] A.M. Ozorio de Almeida and J.H. Hannay, J. Phys. A **20**, 5873 (1987).
[18] M. Kuś, F. Haake and D. Delande, Phys. Rev. Lett. **71**, 2167 (1993); M.W. Biems and G. Alber, Phys. Rev. A **48**, 3123 (1993).
[19] K.M. Atkins and G.S. Ezra, Phys. Rev. A **50**, 93 (1994).
[20] M.V. Berry and M. Tabor, Proc. R. Soc. London A Ser. **349**, 101 (1976).
[21] A.M. Ozorio de Almeida, Lecture Notes. Phys. **263**, 197 (1986).
[22] W.H. Miller, J. Chem. Phys. **56**, 38 (1972); **63**, 996 (1975).
[23] B. Eckhardt and E. Aurell, Europhys. Lett. **9**, 509 (1989).
[24] See, *Chaos and Quantum Physics*, edited by M.-J. Giannoni, A. Voros, and J. Zinn-Justin (Elsevier, New York, 1991); *Quantum Chaos*, Proc. Intl. School Phys. ''Enrico Fermi'' (North–Holland, Amsterdam, 1993).
[25] H. Friedrich and D. Wintgen, Phys. Rep. **183**, 37 (1989).
[26] J.H. Kim and G.S. Ezra, in Proc. Adriatico Conf. *Quantum Chaos*, edited by H.A. Cerdeira, R. Ramaswamy, M.C. Gutzwiller, and G. Casati (World Scientific, Singapore, 1991).
[27] B. Eckhardt, G. Hose, and E. Pollak, Phys. Rev. A **39**, 3776 (1989); G.G. de Polavieja, F. Borondo, and R.M. Benito, Phys. Rev. Lett. **73**, 1613 (1994); K.M. Atkins and G.S. Ezra, Phys. Rev. E **51**, 1822 (1995).
[28] L. Xiao and M.E. Kellman, J. Chem. Phys. **90**, 6086 (1989); Z. Li, L. Xiao and M.E. Kellman, *ibid*. **92**, 2251 (1990); L. Xiao and M.E. Kellman, *ibid*. **93**, 5805 (1990).
[29] S. Neshyba and M.S. Child (unpublished).
[30] M. Baranger, M.R. Haggerty, B. Lauritzen, D.C. Meredith, and D. Provost, CHAOS **5** 261 (1995); see also: E.J. Heller and S. Tomsovic, in *Coherent States: Past, Present and Future*, edited by D. Feng, J.R. Klauder, and M. Strayer (World Scientific, Singapore, 1994). Note also the pioneering application of windowed Fourier transforms to periodic orbit analysis of the ultraviolet absorption spectrum of O_3: B. R. Johnson and J. L. Kinsey, J. Chem. Phys. **91**, 7638 (1989).
[31] S.C. Farantos and L. Zachilas, Mol. Phys. **80**, 1499 (1993).
[32] A.M. Ozorio de Almeida and M.A.M. de Aguiar, Physica D **41**, 391 (1990).
[33] C. Jaffé, J. Chem. Phys. **89**, 3395 (1988).
[34] C. Jaffé and P. Brumer, J. Chem. Phys. **73**, 5646 (1980).
[35] D. Gabor, J. Inst. Electron. Eng. (London) **93**, 429 (1946).
[36] M.V. Berry and K.E. Mount, Rep. Prog. Phys. **35**, 315 (1972).
[37] C.C. Martens and G.S. Ezra, J. Chem. Phys. **87**, 284 (1987).
[38] D.C. Rouben and G.S. Ezra (unpublished).
[39] M. Joyeux, Chem. Phys. **185**, 263 (1994).
[40] E.J. Heller, E.B. Stechel, and M.J. Davis, J. Chem. Phys. **73**, 4720 (1980); M.J. Davis and E.J. Heller, J. Phys. Chem. **75**, 246 (1981).
[41] K.M. Atkins and D. Logan, Phys. Lett. A **162**, 255 (1992); C.C. Martens, J. Stat. Phys. **68**, 207 (1992).
[42] In a paper published after the present research was completed, Liévin *et al*. have computed po period vs energy plots (''vibrograms'') from the Dunham expansion of the vibrational energy levels of the C_2HD molecule, see J. Liévin, M. Abbouti Temsamani, P. Gaspard, and M. Herman, Chem. Phys. **190**, 419 (1995).